Liquid Crystals
Publication details, including instructions for authors and subscription information:
http://www.informaworld.com/smpp/title~content=t713926090

Alternative dynamics for the symmetric splay to bend transition in a nematic liquid crystal layer

Yanli Zhang[a]; David B. Chung[b]; Bin Wang[a]; Philip J. Bos[a]
[a] Liquid Crystal Institute, Kent State University, Kent, OH 44240, USA [b] Intel Corporation, Santa Clara, CA 95052, USA

To cite this Article Zhang, Yanli , Chung, David B. , Wang, Bin and Bos, Philip J.(2007) 'Alternative dynamics for the symmetric splay to bend transition in a nematic liquid crystal layer', Liquid Crystals, 34: 2, 143 — 152
To link to this Article: DOI: 10.1080/02678290601081056
URL: http://dx.doi.org/10.1080/02678290601081056

Liquid Crystals, Vol. 34, No. 2, February 2007, 143–152

Alternative dynamics for the symmetric splay to bend transition in a nematic liquid crystal layer

YANLI ZHANG†, DAVID B. CHUNG‡, BIN WANG† and PHILIP J. BOS†

†Liquid Crystal Institute, Kent State University, Kent, OH 44240, USA
‡Intel Corporation, Santa Clara, CA 95052, USA

A pathway for a coherent topological transition from the splay to bend director configuration in liquid crystal layers has been previously described via order reconstruction in a two-dimensional sheet in the plane of the liquid crystal layer. In this paper we provide the details of the modelling of an alternative pathway that is based on the nucleation, motion and annihilation of an array of disclination lines. Electrical current flow onto the cell is calculated based on the two pathways and compared with data.

1. Introduction

The dynamic switching behaviour of the liquid crystal director field between topologically non-equivalent states is important for liquid crystal devices with the cell geometry shown in figure 1, in which the two surfaces are treated to have pretilt angles of the opposite rotational sense. This director configuration has found application as a bistable display [1, 2], which operates between the two bistable states, splay and twist, and as a fast switching device [3], which works between two bend states after the initial splay to bend transition. The shown bend and twist states are topologically equivalent, while the splay is a topologically distinct state with respect to bend and twist states. It has been shown that the transition between the two topologically distinct states, splay to bend, could occur through the movement of a singular disclination line near the centre or near the surface of the cell [4], or from an 'anchoring-breaking' transition [2, 5].

However, some experimental results could not be explained by these mechanisms. In particular, with the application of a high voltage pulse to the splay state a fast coherent transition, without the apparent motion of a disclination line, can be observed, as was clearly shown by Martinot–Lagarde *et al.* [6] and Barberi *et al.* [7]. They proposed that the coherent transition could be explained as a bulk biaxial melting followed by an order reconstruction in a two-dimensional sheet near the centre of the cell. Martinot–Lagarde *et al.* came to this conclusion through theoretical analysis of the equilibrium states. Barberi *et al.* studied this bulk transition dynamically and explained how the transition depends on the time after the voltage is applied. The pioneering work in these papers explained the phenomenon that previously could not be understood from the model based on the motion of a singular disclination line.

However, the dynamical study was based on a one-dimensional director field, which does not allow the existence of a modulation of the director field in the plane of the cell, or for disclination lines. As was suggested by Marinot–Lagarde, the transient biaxial

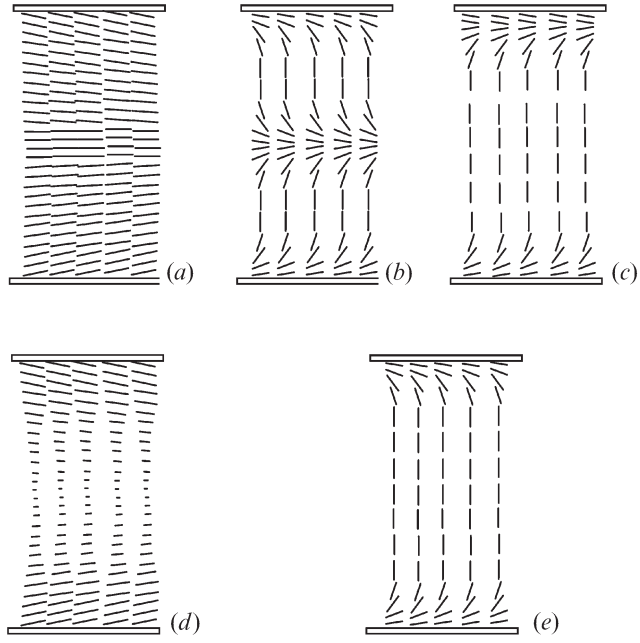

Figure 1. Director configurations in a cell with the shown 'reverse pretilt' alignment. The no-voltage applied splay configuration (*a*), the voltage applied symmetric splay (*b*), and the voltage applied asymmetric splay (*c*), are topologically distinct from the no-voltage twist (*d*) and the voltage applied bend (*e*).

Liquid Crystals
ISSN 0267-8292 print/ISSN 1366-5855 online © 2007 Taylor & Francis
http://www.tandf.co.uk/journals
DOI: 10.1080/02678290601081056

state could be mediated by spinodal decomposition. Following this suggestion, we would like to investigate the type of transition suggested by Martinot–Lagarde using a two-dimensional modelling method. We therefore extend their work by studying the phenomenon of fast bulk transition through a two-dimensional dynamic model. By adding a small perturbation to the system, we observed the nucleation and the motion of an array of disclination lines during the transition at high voltage. We show that this gives a lower energy alternative to the simultaneous order parameter change over a sheet in the centre of the cell.

2. Simulation method

Our model is based on the Laudau–De Gennes free energy representation [8, 9], which is constructed in terms of the Q-tensor, a second rank tensor describing the order parameter of the nematic orientation. It is defined as:

$$Q_{ij} = S\left(n_i n_j - \frac{1}{3}\delta_{ij}\right) \tag{1}$$

where n describes the orientation of the director, and δ_{jk} is the Kronecker tensor, which is 1 if the two subscripts are alike, and 0 otherwise. S is the scalar order parameter, defined from the microscopic approach as:

$$S = \frac{1}{2}\langle\left(3\cos^2\theta - 1\right)\rangle \tag{2}$$

where θ is the polar angle of molecular orientations **u** with the director **n**.

In our simulation, the Laudau–De Gennes free energy density expression, is composed of three parts [10–13]: thermal energy f_T, elastic energy f_S, and electric energy f_V:

$$f_T = f_0 + A(T - T^*)Q_{ij}Q_{ji} - BQ_{ij}Q_{jk}Q_{ki} + C\left(Q_{ij}Q_{ij}\right)^2 + O\left(Q^5\right)$$

$$f_S = \frac{1}{S_o^2}\left[\frac{1}{12}(K_{33} - K_{11} + 3K_{22})G_1^{(2)} + \frac{1}{2}(K_{11} - K_{22} + 3K_{24})G_2^{(2)} + \frac{1}{2}K_{24}G_3^{(2)} + \frac{1}{6}(K_{33} - K_{11})G_6^{(3)} + q_0K_{22}G_4^{(2)}\right]$$

$$G_1^{(2)} = Q_{jk,\,l}Q_{jk,\,l} \quad G_2^{(2)} = Q_{jk,\,k}Q_{jl,\,l} \quad G_3^{(2)} = Q_{jk,\,k}Q_{jl,\,k}$$

$$G_4^{(2)} = e_{jkl}Q_{jm}Q_{jm,\,l} \quad G_6^{(3)} = Q_{jk}Q_{jm,\,j}Q_{jm,\,k}$$

$$f_V = -\frac{1}{2}\varepsilon_0\left(\bar{\varepsilon}V_j^2 + \Delta\varepsilon V_{,j}V_{,k}\frac{Q_{jk}}{S_0}\right). \tag{3}$$

where $\bar{\varepsilon} = \frac{2\varepsilon_\perp + \varepsilon_\parallel}{3}$, $\Delta\varepsilon = \varepsilon_\perp - \varepsilon_\parallel$, $V_{,j} = \frac{\partial V}{\partial j}$

The factor S_0 is a value of S where the elastic constants and dielectric anisotropy were measured. In our calculations, it is a constant set as 0.6656. For the elastic term, Schiele and Trimper [14] have shown that using only one 3rd order term in derivatives of Q tensor $G_6^{(3)}$ is sufficient to lift the degeneracy between K_{11} and K_{33}.

Our numerical relaxation method is based on the dynamic equation:

$$\gamma\frac{\Delta Q_{jk}}{\Delta t} = -\left[f_g\right]_{Q_{jk}} \tag{4}$$

where γ is the viscosity, f_g is the total free energy of the three parts: thermal, elastic and electric energy. $\left[f_g\right]_{Q_{jk}}$ is the functional derivative calculated as follows:

$$\left[f_g\right]_{Q_{jk}} = \frac{\partial f_g}{\partial Q_{jk}} - \frac{\mathrm{d}}{\mathrm{d}x}\left(\frac{\partial f}{\partial Q_{jk,\,x}}\right) - \frac{\mathrm{d}}{\mathrm{d}y}\left(\frac{\partial f}{\partial Q_{jk,\,y}}\right) - \frac{\mathrm{d}}{\mathrm{d}z}\left(\frac{\partial f}{\partial Q_{jk,\,z}}\right). \tag{5}$$

The functional derivatives of the three free energy components take the following forms:

$$\begin{aligned}
\left[f_T\right]_{Q_{jk}} &= 2A(T - T^*)Q_{jk} - 3BQ_{ji}Q_{ik} + 4CQ_{jl}Q_{li}Q_{ik} \\
\left[f_s\right]_{Q_{jk}} &= \frac{1}{S^2}\Bigg[-2\left(-\frac{1}{12}K_{11} + \frac{1}{4}K_{22} + \frac{1}{12}K_{33}\right)Q_{jk,\,ll} \\
&\quad + (K_{11} - K_{22})Q_{jl,\,lk} - K_{24}Q_{jl,\,lk} + \frac{1}{4}(K_{33} - K_{11}) \\
&\quad \left(Q_{lm,\,j}Q_{lm,\,k} - Q_{lm,\,l}Q_{jk,\,m} - Q_{lm}Q_{jk,\,ml}\right. \\
&\quad \left. - Q_{lm,\,m}Q_{jk,\,l} - Q_{lm}Q_{jk,\,lm}\right) + 2q_0K_{22}e_{jlm}Q_{mk,\,l}\Bigg] \\
\left[f_V\right]_{Q_{jk}} &= -\frac{1}{2S}\varepsilon_0\Delta\varepsilon V_{,j}V_{,k}.
\end{aligned} \tag{6}$$

In our simulation, infinite anchoring is assumed, that is, the Q-tensors at the two boundaries are fixed and are constructed from equation (1) by assuming the initial value $S = 0.6$.

To ensure the validity of the simulation result, we carried out a series of tests of our Q-tensor program before proceeding to perform the simulation on the transition between topologically distinct states from splay to bend at high voltage. First, we checked the temperature term under the condition of no applied voltage and a uniform director distribution. In this case, the contributions from the voltage and strain terms to the functional derivative are zero. The phase transition from nematic to isotropic is of the first order, therefore the order parameter changes abruptly at the transition temperature T_{NI}, This behaviour of the order parameter with temperature serves as a good check for the temperature term in the program.

The temperature terms A, B, C, $T_{NI} - T^*$ and the order parameter S at T_{NI} are related to each other. The temperature term of the Landau–De Gennes free energy in terms of S based on equation (3) takes the form:

$$f_g = f_0 + \frac{2}{3}A(T - T^*)S^2 - \frac{2}{9}BS^3 + \frac{2}{9}CS^4. \tag{7}$$

Minimizing the f_g, and given the condition that $f_g=f_0$ at $T=T_{NI}$, we can derive:

$$S_{NI}=\frac{B}{2C}$$
$$T_{NI}-T^*=\frac{B^2}{12AC}. \quad (8)$$

One of the simulation difficulties of the Q-tensor method is the lack of the available parameters for temperature terms. We take the A, B, C values of liquid crystal material 5CB from reference [15]: $A=0.0975\times10^6\,\mathrm{J\,k^{-1}\,m^{-3}}$, $B=2.4\times10^6\,\mathrm{J\,m^{-3}}$, $C=4.3875\times10^6\,\mathrm{J\,m^{-3}}$, and $T_{NJ}-T^*=1.1^\circ$C, $T_{NI}=35.2^\circ$C, which is also same as in the paper by Barberi [7]. (The values appear different from [7] due to the different form used for the temperature term.)

The elastic constants of 5CB used in simulations are: $K_{11}=6.3$ pN, $K_{22}=3$ pN, $K_{33}=9$ pN, and the dielectric constants of 5CB are $\varepsilon_{\|}=20$, and $\varepsilon_{\perp}=5$. No chiral agent is considered. After the relaxation, S is calculated from the following equation [16]:

$$S=1.5[\mathrm{tr}\,(Q\cdot Q)]^{\frac{1}{2}}. \quad (9)$$

The calculated order parameters at different temperatures are plotted in figure 2. The calculated S_{NI} by program is the same as that predicated from equation (8).

To check the stain and voltage term, we compare the one-dimensional director profile of the electrically controlled birefringence (ECB) cell at a certain voltage

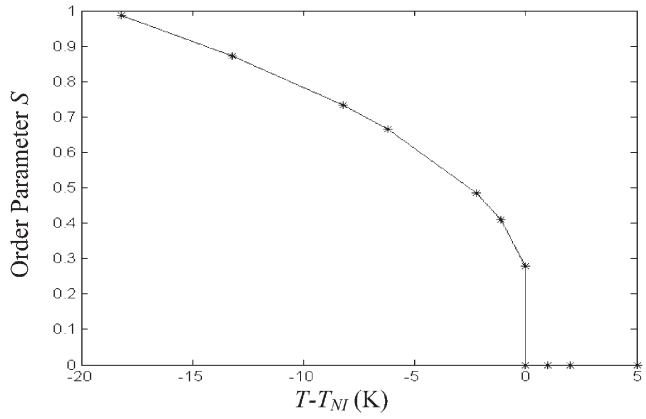

Figure 2. Temperature dependence of the scalar order parameter, S.

obtained by the Q-tensor method and vector method [12] at a fixed temperature (29°) below the isotropic–nematic transition. The comparison result of the director profile across the cell thickness direction is shown in figure 3.

We see that the two methods agree well in the bulk, except at the boundary. This might due to the incorrect setting of S at the boundary that affects the Q-tensor value and director profile correspondingly at the two boundary layers. We also observe that the two methods agree better at higher voltage, since at higher voltages the boundary layer is thinner. We consider that our Q-tensor program is at least valid to study the splay to bend transition at voltages above 10 V.

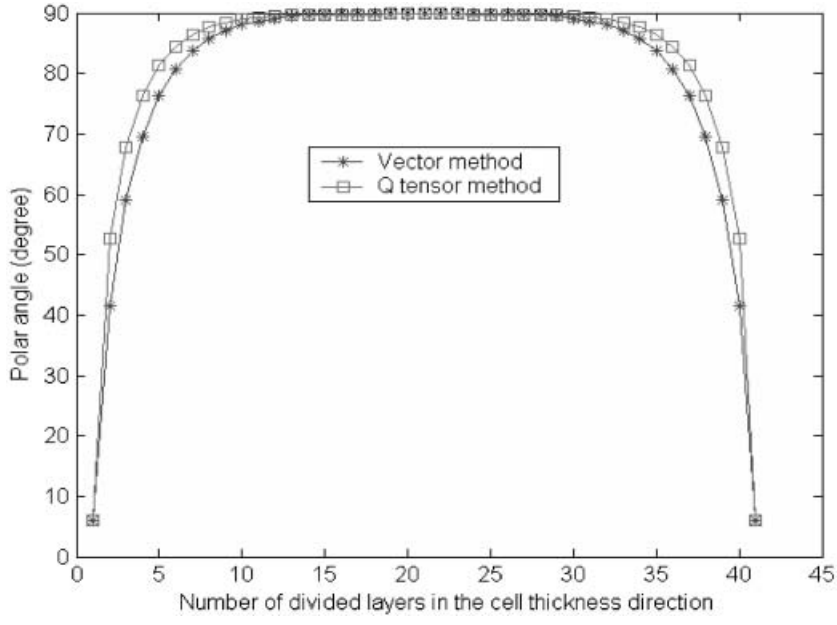

Figure 3. Comparison of director profiles of a ECB cell at 5 V obtained by vector method and Q-tensor method.

The modelled liquid crystal layer was 1 μm thick and 2 μm wide. The electrodes are un-patterned and lie along the top and bottom surfaces of the layer. The initial state is a splay state with the pretilt angle being of the opposite rotational sense on the two surfaces; the initial director profile of the splay state is obtained by linear extrapolation from the two surface pretilt angles fixed as 6°. In this case, the director angle of the middle layer is extrapolated as 0°. However, in the real cell, due to the existence of the spacers or a small difference of the pretilt angles at the two surfaces or thermal fluctuations, the pretilt angle at the middle layer of the cell will not be exactly 0° everywhere. Therefore, we add a perturbation to the initial condition of the cell configuration by setting the angle at the middle layer to follow a sinusoidal function with 1° amplitude and 2 μm period, as shown in figure 4 (the angles in the middle layer are exaggerated) [17].

To study the time dependence of the transition, the dynamic relaxing method, instead of the method to find the equilibrium state, is applied in the modelling [11]. The stop condition is controlled by the relaxation time with the time step $\Delta t = 10^{-9}$s. To stabilize the calculation, the viscosity γ of the liquid crystal is set as 0.1 Pa s in the program.

Variation of the order parameter may be induced in regions of very high elastic distortion. However, this variation is only expected to be observed over very short distances. Therefore a very fine grid spacing, of the order of a molecular length, is needed for the simulation. If we apply the fine grid spacing to the whole cell, a very large number of grid points is needed, which is memory and time consuming. To solve this problem, we developed a coarse–fine grid scheme for the simulation. Theoretically, we know the order parameter decreases only at the region where the elastic distortion energy is high. In the case of a splay to bend transition, this region will be the splay wall in the centre of the cell. Therefore, we apply a fine grid only to that region, and at each time step the coarse and fine grid regions are correlated with each other through the boundary values.

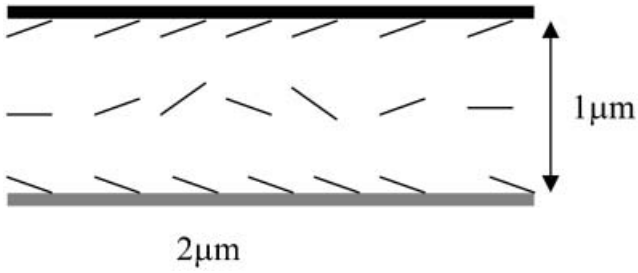

Figure 4. The perturbation scheme in the initial condition of Pi cell.

3. Results

The order parameter and director field evolution are shown as functions of time in figures 5–10. The time referred to is the time after the application of an 18 v potential at 29°C to the cell electrodes. As mentioned above, the initial condition for this relaxation scenario is where the director was determined by first linear extrapolation from the polar angle of the director on the top surface to that on the lower surface; the directors for the layer of the central grid points are then modulated with the sinusoidal wave function $A \sin(2\pi x/p)$, as discussed in § 2, where A is the amplitude, P is the total grid number in the cell width direction, and x is the grid number in the cell width direction. The director in the middle layer is only fixed by this condition for the first time step of the calculation (10^{-9} s).

As Figure 5 and 6 [17] demonstrate, immediately after the voltage is applied to the cell, the perturbation in the middle layer grows, and a region of a

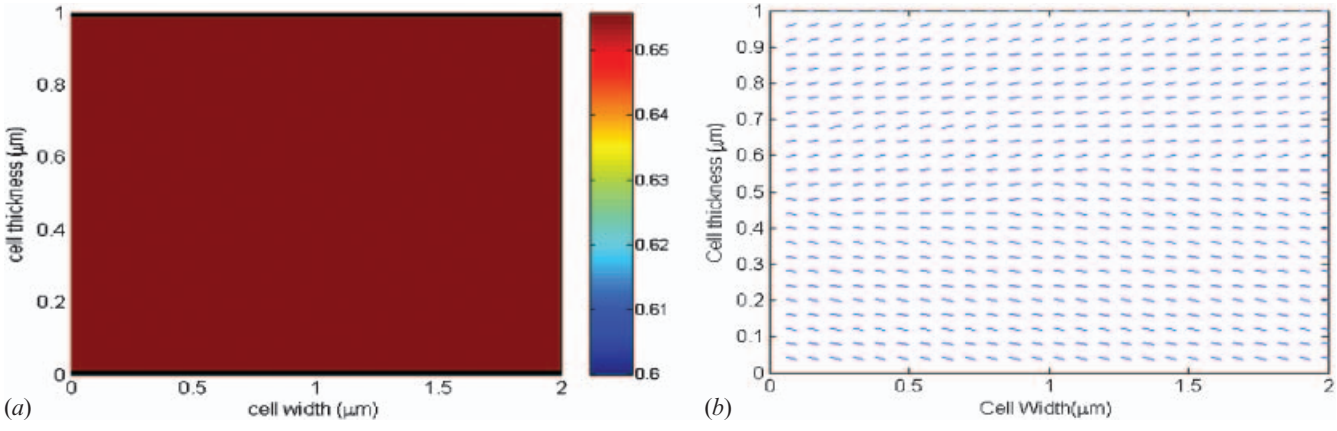

(a) (b)

Figure 5. (a) Order parameter profile at 0.6 μs; (b) director profile at 0.6 μs.

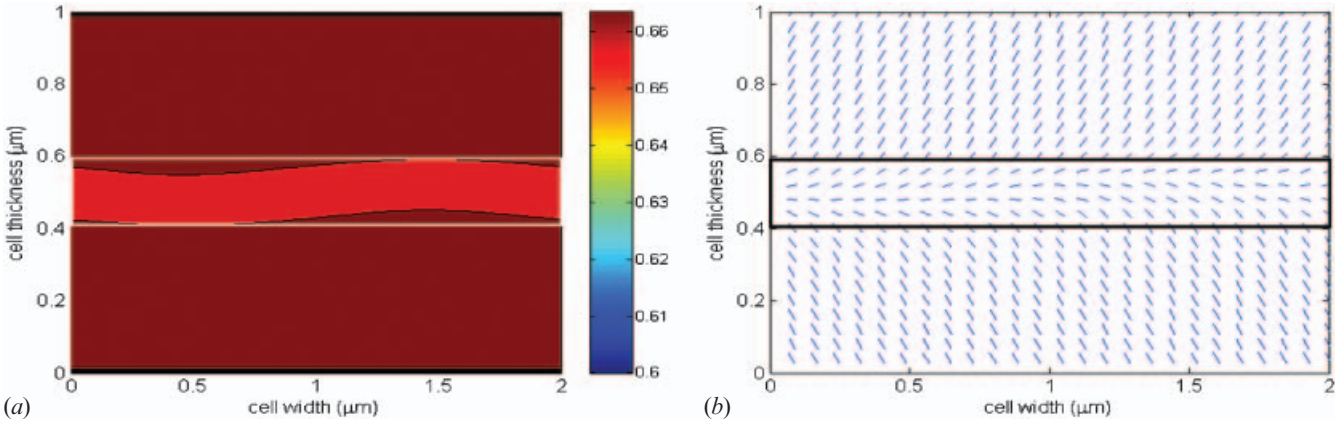

Figure 6. (*a*) Order parameter profile at 15 μs; (*b*). director profile at 15 μs.

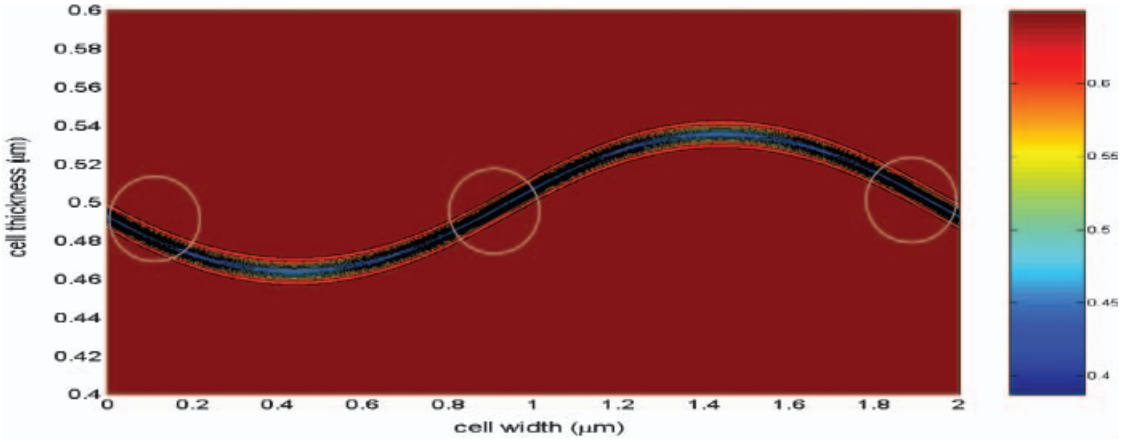

Figure 7. Order parameter profile in the fine grid area at 30.2 μs.

concentrated splay distortion is formed at the middle of the layer, as outlined by the box in figure 6. In the figures of order parameter profile, the colour is related to the order parameter value as defined by the colour bar on the right. The area inside the box in figure 6 has the highest elastic energy distortion of the cell, and is the place where the order parameter is expected to vary; therefore, we apply fine grids of 1 nm spacing to this area. Figures 7–9 [17] show only this central region of the cell, which is 200 nm thick. Figures 10 (*a*) and 10 (*b*) [17] show the final state of the whole cell after the transition.

These simulation results clearly show that the transition in this case is through the nucleation and motion of an array of disclination lines. After the region of concentrated splay distortion is formed, the order parameter begins to decrease in that region. However, the amount of decrease is non-uniform, and at about 30.2 μs groups of defect cores are generated at the regions marked in figure 7, which represent the end view of lines running perpendicular to the plane of the figures. We then observe in the figures generated as a function of time, that each of the original defect cores evolves to a pair of −1/2 and +1/2 disclination lines that move away from each other toward other defect lines with the opposite sign. In this way the topology of the cell is changed from the splay state to the bend state. Finally the −1/2 and +1/2 disclination lines annihilate each other, completing the transition, as shown in figures 10 (*a*) and 10 (*b*).

4. Discussion

In [7] an explanation of the splay to bend transition is gived based on a one-dimensional calculation predicting that the transition could occur via an order parameter change over a two dimensional sheet in the centre of the cell. This previous work led to a rather poor fit of the shape of the charging current vs. time curve, as shown from figures 11 and 12 taken from [7]. Comparing

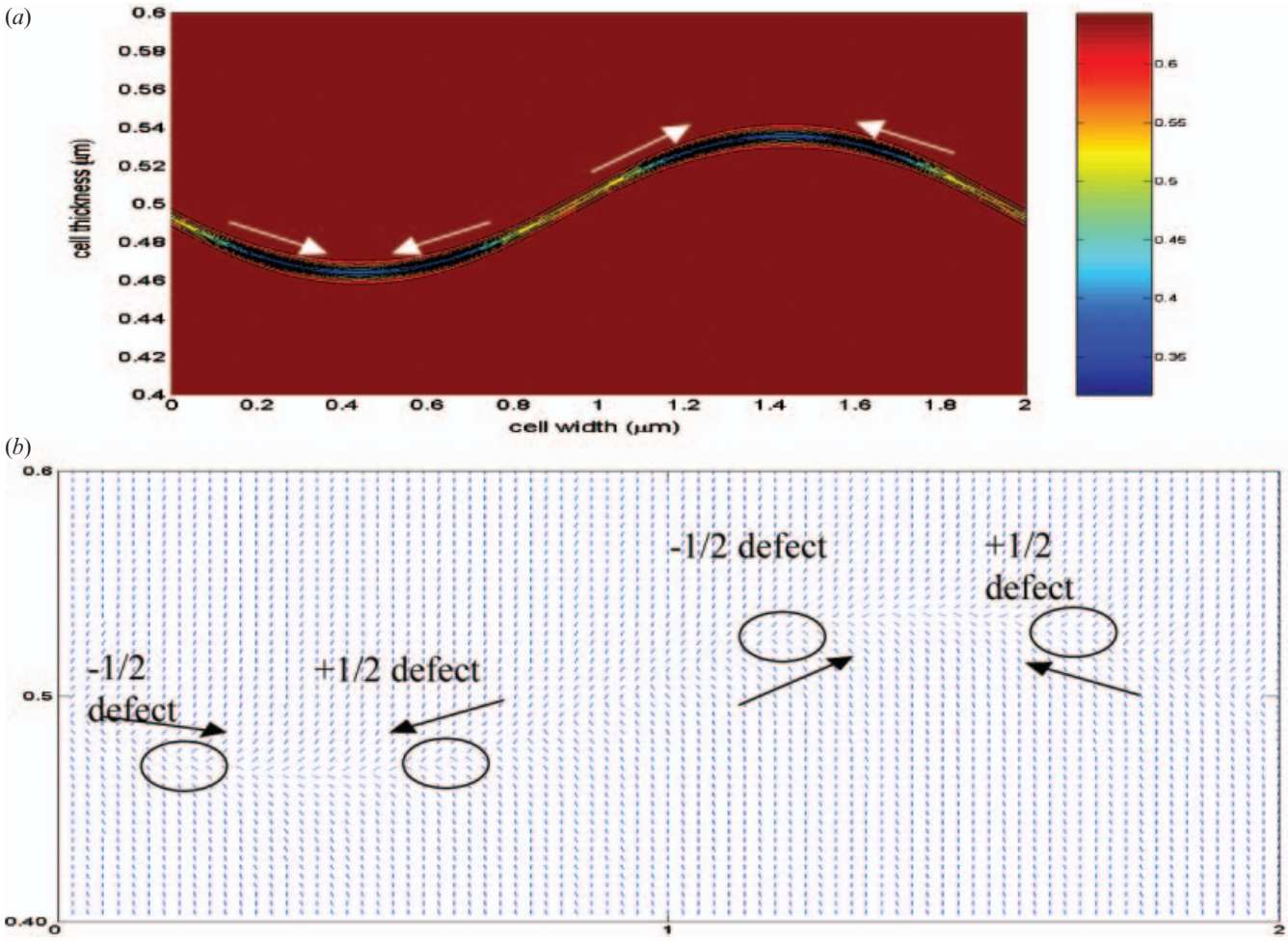

Figure 8. (*a*) Order parameter profile in the fine grid area at 30.4 μs; (*b*) director profile in the fine grid area at 30.4 μs.

figures 11 and 12, we note that the second peak in the experimental result is much lower and broader than that in the simulation result.

Our method is different in that it allows for a two-dimensional director configuration, which allows the possibility of the transition to occur via the motion of an array of disclination lines. Our simulated current vs. time curve, which is shown in figure 13 [17], agrees much better with the experiment result. We would like to point out here that the curve in figure 13 is based on one perturbation mode, and in the real system, there would co-exist different modes with different perturbation periods and amplitudes; the longer perturbation period will lead to a lower and broader second peak, which will bring closer agreement between our simulation result of the current curve agree and the experimental result. The current in figures 13 and 14 is calculated as being proportional to $d\bar{\varepsilon}/dt$, where $\bar{\varepsilon}$ is an average of the dielectric constants over rows and columns in our two-dimensional calculation.

We also performed the simulation without the introduction of a perturbation to the mid layer director tilt angle, which is similar to the one-dimensional simulation by Barberi *et al.* The result is shown in figure 14. In this case, we also observed the bulk order reconstruction transition predicted by Barberi *et al.* However, this transition happens at a later time than that through the nucleation and motion of an array of disclinations at the same voltage. This indicates that the transition through the defect nucleation and disclination line movement happens preferentially over the bulk order reconstruction based transition.

To understand how even a very slight perturbation considered here can cause the transition to occur through defect nucleation and motion, as opposed to the order reconstruction in a two-dimensional sheet, it is helpful to look at figure 15(*a*), which shows the director profile at 29 μs, which is before the nucleation of defect core; the magnified director profiles are shown in figures 15 (*b*) and 15 (*c*). It is clear that the elastic

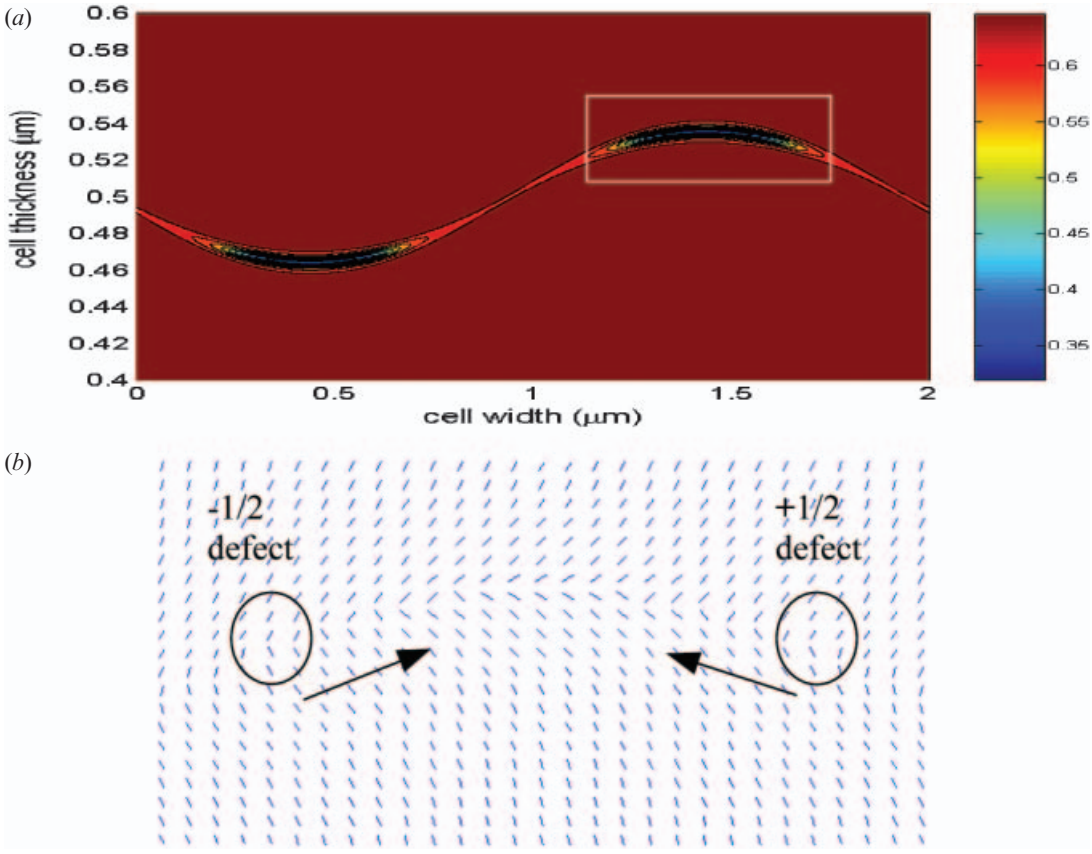

Figure 9. (*a*) Order parameter profile in the fine grid area at 30.8 μs; (*b*) director profile inside the box of figure 7 (*a*) at 30.8 μs.

distortion in area 1 is higher than in area 2, so we can expect the defect to be generated in area 1 first. We note that the director profile of area 2 is similar to the case without perturbation.

In this modelling we have considered the case where the initial director field is completely uniform and symmetric, but also where a slight perturbation is introduced. This perturbation was very small, with only a 1° amplitude, and a periodicity of 2 μm. These values can be justified from the amplitude expected for thermal director fluctuations. The average amplitude of thermally induced fluctuation can be estimated from the following equation [18]:

$$\langle \delta\theta^2 \rangle = \frac{K_B T}{Kd}$$

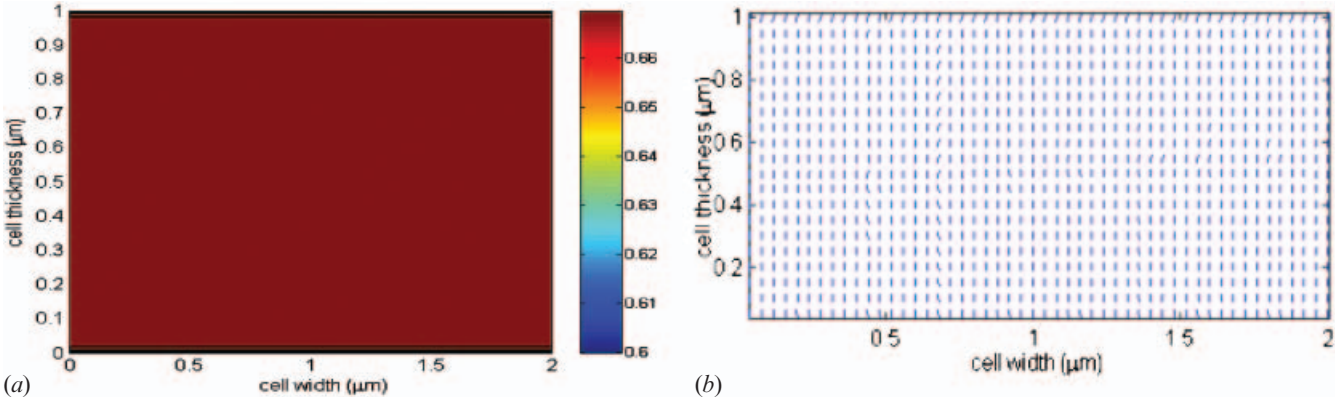

Figure 10. (*a*) Order parameter profile at 36 μs; (*b*) director profile at 36 μs.

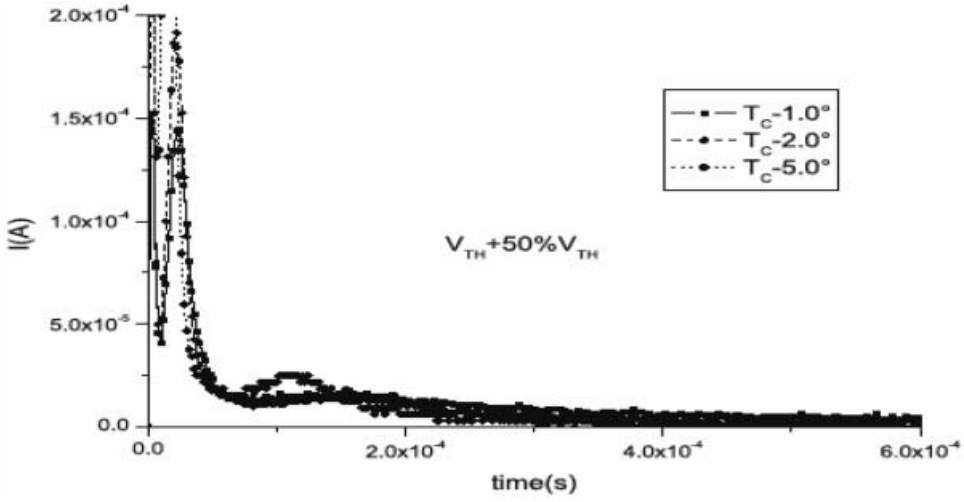

Figure 11. Experimental result by Barberi *et al.* Current during a pulse with voltage 50% above the threshold.

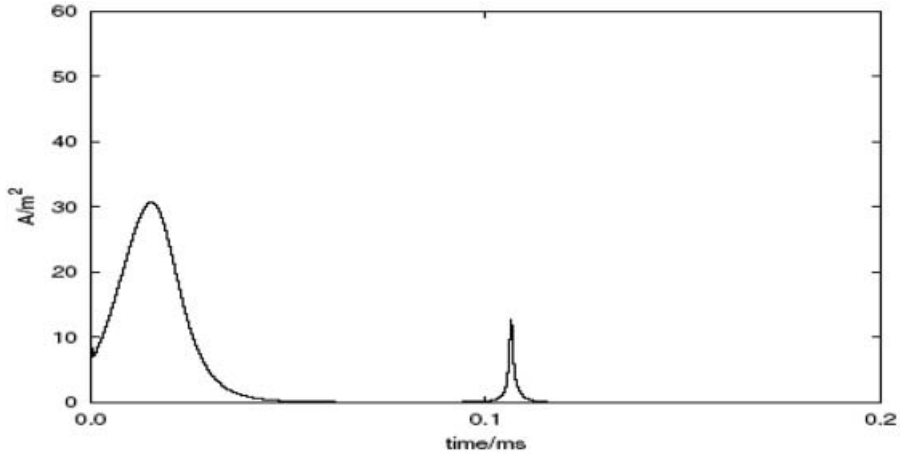

Figure 12. Simulation result by Barberi *et al.* Current density across the cell during the switching process.

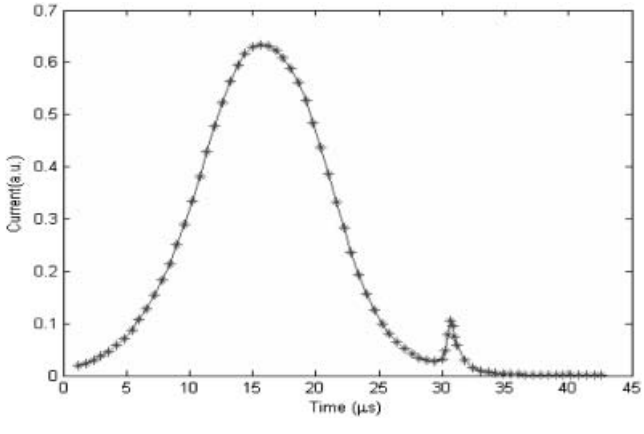

Figure 13. Current density across the cell during the switching process at 18 V with initial perturbation in the middle layer.

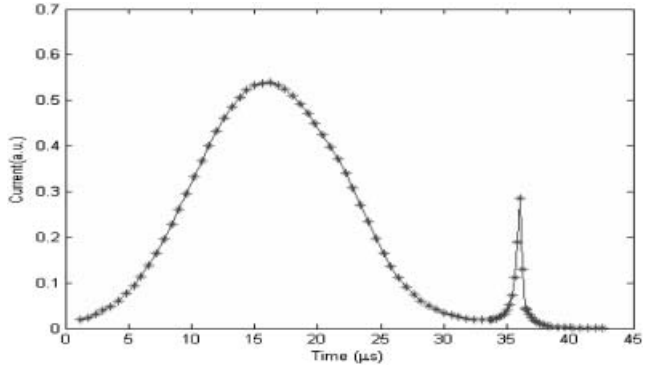

Figure 14. Current density across the cell during the switching process at 18 V without perturbation.

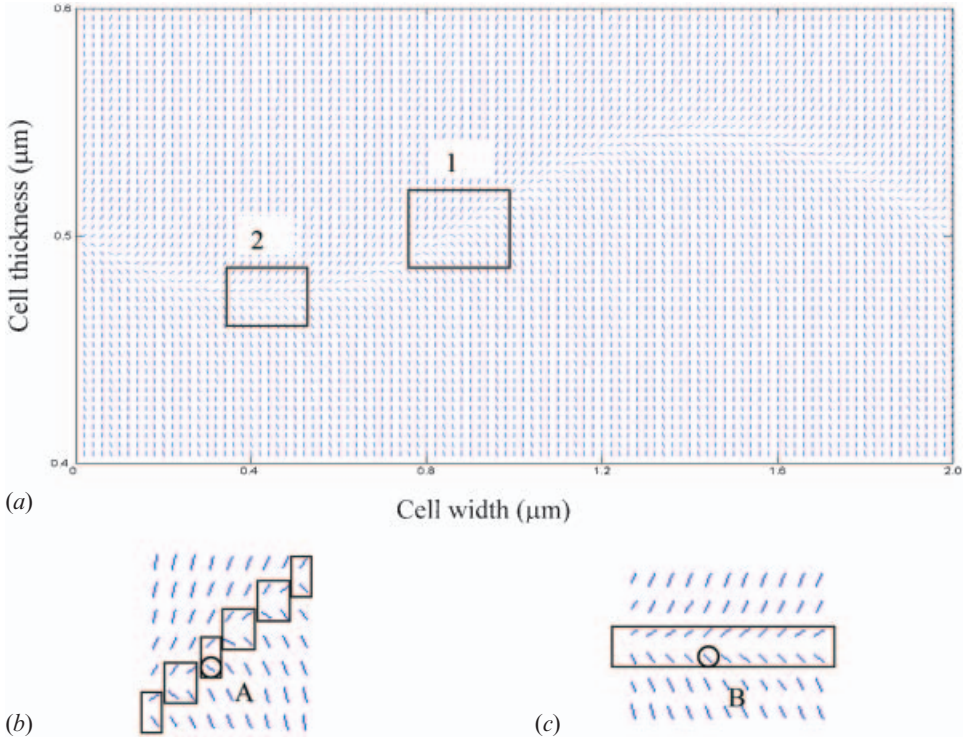

Figure 15. (*a*) Director profile in the fine grid area at 29 μs at 18 V with perturbation; (*b*) director profile inside box 1; (*c*) director profile inside box 2.

where K_B is the Boltzmann constant, K is the elastic constant and d is the cell gap. If we use $T=300\,\mathrm{K}$, $K=10\times10^{-12}\,\mathrm{N}$, $d=1\,\mu\mathrm{m}$, then $\delta\theta$ is about 20 mrad, which is about 1.1°. We do not cause any stabilization of this perturbation, as it is only the initial condition. If it was energetically unfavourable, it would be expected to die away. That it does grow verifies that the uniform distortion in the centre of the cell is unstable to the particular perturbation that we considered. Our result does not prove that the particular selected periodicity will be the fastest growing mode, or the one that is observed, but makes it very probable, given the wide spectrum of thermal director fluctuations, that some thermal mode will cause the uniform state to be unstable

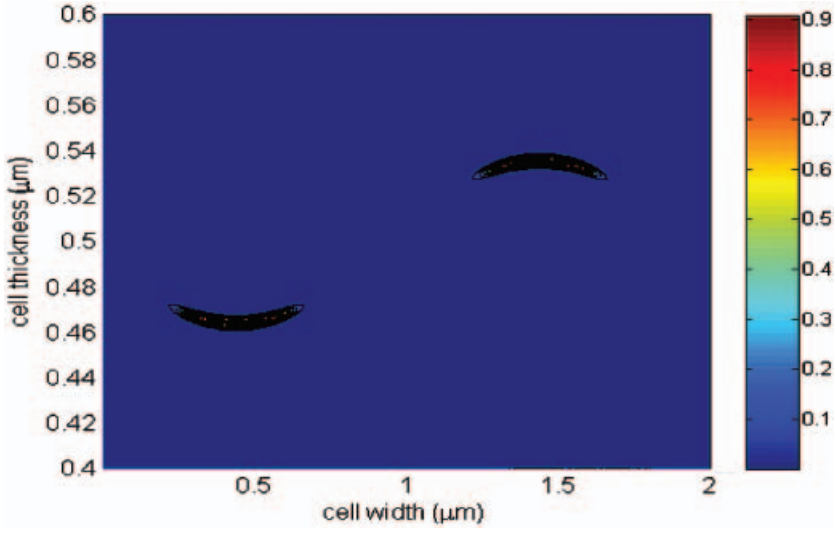

Figure 16. Biaxiality profile in the fine grid area at 30.8 μs.

Barbari *et al.* [19] showed that the time at which the transition occurs is about 80 µs. However more complete data by Joly *et al.* [20] provide the time where the transition begins, and also the time required for the transition to occur, as a function of voltage. For the conditions of their experiment and for an applied voltage of 18 V, these times are about 25 and 1.5 µs, respectively. Given the difference between the experimental results in these two studies, our simulation values of about 30 and 1 µs, respectively, are within the expected range.

Finally, we would like to point out that we also checked the biaxiality of the defect core structure following the same method used by Barberi *et al.* [7]. The biaxiality is measured by an invariant b, which is defined as [21]:

$$b^2 = 1 - \frac{6\,\mathrm{tr}\,(Q^3)^2}{\mathrm{tr}\,(Q^2)^3}, \quad b \in [0, 1].$$

In uniaxial states $b=0$, in biaxial states $b\neq 0$, and the maximum value $b=1$ is attained when $\mathrm{tr}\,(Q^3)=0$, which occurs when Q has one zero eigenvalue and two eigenvalues with equal moduli and opposite signs. We found the same result from our simulation as found by Barberi *et al.*; that is, the biaxiality is maximum just around the defect core as shown in figure 16.

We wish to emphasize in this paper that there is an alternative transition pathway to the one-dimensional analysis previously presented However we would like to make clear that more complicated processes could be expected in a real 3D cell, which cannot be simulated by our 2D model. We would expect, based on our 2D modelling, that in the real 3D cell an instability of some type would form, and it will cause the localization of defect lines.

5. Conclusion

A coherent transition from the splay to bend state resulting from the application of a high voltage to a layer of liquid crystalline material has been previously observed experimentally, and explained as an order reconstruction in a two-dimensional sheet near the centre of the layer through a one dimensional model. We studied this splay to bend transition at high voltages through a 2D dynamic model. Our simulation results show that, with the introduction of perturbations, the transition can take place through the nucleation and motion of an array of disclination lines in the bulk of the cell. This transition occurs preferentially over the two-dimensional bulk sheet melting predicted by the one-dimensional modelling.

References

[1] G.D. Boyd, J. Cheng, P.D.T. Ngo. *Appl. Phys. Lett.*, **36**, 556 (1980).
[2] I. Dozov, M. Nobili, G. Durand. *Appl. Phys. Lett.*, **70**, 1179 (1997).
[3] P.J. Bos, R.K. Koehler/Beran. *Mol. Cryst. liq. Cryst.*, **113**, 329 (1984).
[4] H. Nakamura, M. Noguchi. *Jpn. J. appl.Phys.*, **39**, 6368 (2000).
[5] I. Dozov, G. Durand. *Liq. Crys. Today*, **8**, 1 (1998).
[6] Ph. Martinot-Lagarde, H. Dreyfus-Lambez, I. Dozov. *Phys. Rev. E*, **67**, 051710 (2003).
[7] R. Barberi, F. Ciuchi, G.E. Durand, M. Iovane, D. Sikharulidze, A.M. Sonnet, E.G. Virga. *Eur. Phys. J. E*, **13**, 61 (2004).
[8] P.G. De Gennes. *Mol. Cryst. liq. Cryst.*, **12**, 193 (1971).
[9] D.W. Berreman, S. Meiboom. *Phys. Rev. A*, **30**, 1955 (1984).
[10] S. Dickmann. PhD thesis, Univeristy of Karlsruhe, Germany (1995).
[11] H. Mori, E.C. Gartland, Jr, J.R. Kelly, P.J. Bos. *Jpn. J. appl. Phys.*, **38**, 135 (1999).
[12] J.E. Anderson, P.E. Watson, P.J. Bos. *Liquid Crystal Display 3-D Director Simulator Software and Technology Guide*. Artech, Norwood, Massachusetts (2001).
[13] G.D. Lee, J.E. Anderson, P.J. Bos. *Appl. Phys. Lett.*, **81**, 3951 (2002).
[14] K. Schiele, S. Trimper. *Phys. Status Solidi B*, **118**, 267 (1983).
[15] H. Coles. *Mol. Crys. liq. Cryst. Lett.*, **49**, 67 (1978).
[16] O.D. Lavrentovich, P. Pasini, C. Zannoni, S. Zumer. *Defects in Liquid Crystals: Computer Simulations, Theory and Experiments*, pp. 17–36, Klumer Academic Publishers (2000).
[17] Y. Zhang, B. Wang, D. Chung, J. Colegrove, P. Bos. *SID Symp. Dig.*, **36**, 1782 (2005).
[18] U. Bisang, G. Ahlers. *Phys. Rev. Lett.*, **80**, 3061 (1998).
[19] R. Barberi, F. Ciuchi, G. Lombardo, R. Bartolino, G.E. Durand. *Phys. Rev. Lett.*, **93**, 137801-1 (2004).
[20] S. Joly, I. Dozov, Ph. Martinot-Lagarde. *Phys.Rev.Lett.*, **96**, 019801 (2006).
[21] P. Kaiser, W. Wiese, S. Hess. *J. non-equilib. Thermodyn.*, **17**, 153 (1992).